THE JOURNAL OF BIOLOGICAL CHEMISTRY VOL. 282, NO. 30, pp. 22112–22121, July 27, 2007

Structural Mechanism for Substrate Inhibition of the Adenosine 5′-Phosphosulfate Kinase Domain of Human 3′-Phosphoadenosine 5′-Phosphosulfate Synthetase 1 and Its Ramifications for Enzyme Regulation*[S]

Received for publication, February 27, 2007, and in revised form, May 8, 2007 Published, JBC Papers in Press, May 31, 2007, DOI 10.1074/jbc.M701713200

Nikolina Sekulic[‡1], **Manfred Konrad**[§2], **and Arnon Lavie**[‡1,3]

From the [‡]*Department of Biochemistry and Molecular Genetics, University of Illinois, Chicago, Illinois 60607 and the* [§]*Max Planck Institute for Biophysical Chemistry, Göttingen D-37077, Germany*

In mammals, the universal sulfuryl group donor molecule 3′-phosphoadenosine 5′-phosphosulfate (PAPS) is synthesized in two steps by a bifunctional enzyme called PAPS synthetase. The APS kinase domain of PAPS synthetase catalyzes the second step in which APS, the product of the ATP-sulfurylase domain, is phosphorylated on its 3′-hydroxyl group to yield PAPS. The substrate APS acts as a strong uncompetitive inhibitor of the APS kinase reaction. We generated truncated and point mutants of the APS kinase domain that are active but devoid of substrate inhibition. Structural analysis of these mutant enzymes reveals the intrasubunit rearrangements that occur upon substrate binding. We also observe intersubunit rearrangements in this dimeric enzyme that result in asymmetry between the two monomers. Our work elucidates the structural elements required for the ability of the substrate APS to inhibit the reaction at micromolar concentrations. Because the ATP-sulfurylase domain of PAPS synthetase influences these elements in the APS kinase domain, we propose that this could be a communication mechanism between the two domains of the bifunctional enzyme.

Enzyme inhibitors are molecules that bind to enzymes and decrease their activity. Usually, we think of inhibitors as molecules that mimic the substrates, products, or transition state or fit in an allosteric site and, once bound, arrest the enzyme in its catalytic cycle or slow it down. However, even the true substrates (or products) of the reaction can act as inhibitors. In such cases, enzyme kinetic measurements show pronounced deviations from the hyperbolic dependence of velocity on substrate concentration. Substrate inhibition is usually observed only at high substrate concentrations, whereas at low substrate concentrations the kinetics follow simple Michaelis-Menten behavior.

Substrate or product inhibition phenomena are widely found in nature and believed to be important for metabolic feedback regulation processes (1–3). However, the underlying mechanisms are complex and structurally poorly characterized. In this work, we shed light on one such system present in adenosine 5′-phosphosulfate (APS)[4] kinase.

APS kinase is an evolutionarily conserved enzyme catalyzing the second step in the formation of 3′-phosphoadenosine 5′-phosphosulfate (PAPS), the universal sulfuryl donor in biological systems. In the first reaction of PAPS formation, inorganic sulfate is converted to APS by ATP-sulfurylase. In the second reaction, APS kinase phosphorylates APS at the 3′-hydroxyl of the ribose to produce PAPS.

$$\text{ATP-Mg} + SO_4^{2-} \rightleftharpoons \text{APS} + PP_i\text{-Mg (ATP sulfurylase)}$$
REACTION 1

$$\text{APS} + \text{ATP-Mg} \rightleftharpoons \text{PAPS} + \text{ADP-Mg (APS kinase)}$$
REACTION 2

PAPS is used as a substrate for sulfotransferases, which sulfonate a wide rage of molecules, including proteins, glycosaminoglycans, steroid hormones, and xenobiotics (4). ATP-sulfurylase and APS kinase are separate enzymes in bacteria, yeast, fungi, and plants, but are found on a single polypeptide chain in the animal kingdom (5). In its bifunctional form, called PAPS synthetase or PAPSS, each domain retains the same fold as in the homologous monofunctional enzyme (6–8). The significance of this protein fusion is still ambiguous. Kinetic studies indicate no substrate channeling between the domains (9), a result consistent with the recent crystal structure of human PAPSS (8).

The importance of the reaction catalyzed by PAPSS is emphasized by the fact that mutations in one of the two iso-

* Use of the Advanced Photon Source was supported by the U. S. Department of Energy, Office of Science, Office of Basic Energy Sciences, under Contract W-31-109-Eng-38. The costs of publication of this article were defrayed in part by the payment of page charges. This article must therefore be hereby marked "*advertisement*" in accordance with 18 U.S.C. Section 1734 solely to indicate this fact.

The atomic coordinates and structure factors (code 2pey and 2pez) have been deposited in the Protein Data Bank, Research Collaboratory for Structural Bioinformatics, Rutgers University, New Brunswick, NJ (http://www.rcsb.org/).

[S] The on-line version of this article (available at http://www.jbc.org) contains supplemental Figs. S1–S4.

[1] Supported by National Institutes of Health Grant AI046943.

[2] Supported by the Max-Planck Society.

[3] To whom correspondence should be addressed: Dept. of Biochemistry and Molecular Genetics, 900 South Ashland Ave., MBRB Room 1108, University of Illinois, Chicago, IL 60607. Tel.: 312-355-5029; Fax: 312-355-4535; E-mail: lavie@uic.edu.

[4] The abbreviations used are: APS, adenosine 5′-phosphosulfate; PAPS, 3′-phosphoadenosine 5′-phosphosulfate; PAPSS, PAPS synthetase; Δ25N, Δ34N, and Δ50N, the truncation mutants of the APS kinase domain of human PAPSS1 that start at residues 26, 35, and 51, respectively, and end at residue 227; d-, deoxy-; RB1, rigid body 1; RB2, rigid body 2; GST, glutathione *S*-transferase; NMP, nucleoside monophosphate.

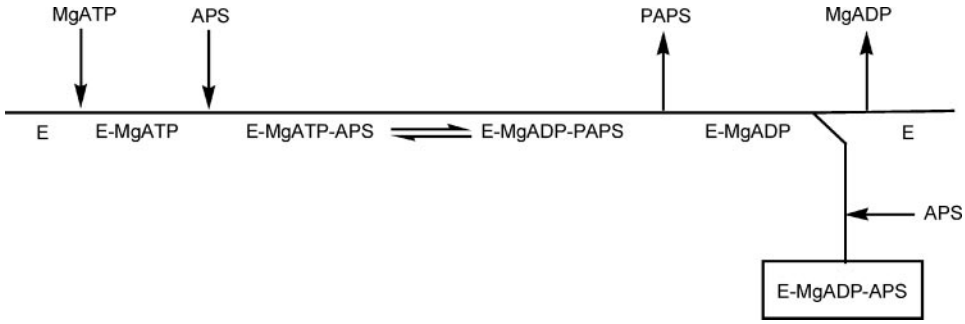

SCHEME 1. **The ordered binding kinetic mechanism of APS kinase.** The inhibitory complex (*E*·MgADP·APS) is formed after release of the product PAPS by the enzyme (*E*), to which APS binds prior to ADP release.

forms of this enzyme (PAPSS1 and PAPSS2) significantly affect phenotype. Mutation in isoform 2 (PAPSS2) is associated with spondyloepimetaphyseal dysplasia disease in humans (10) and brachymorphism in mice (11, 12).

Extensive biochemical studies on the *Penicillium chrysogenum* (13) APS kinase have revealed that this enzyme forms a dimer in solution and follows a sequential ordered reaction mechanism: the substrate MgATP binds before APS, and the release of the product PAPS occurs prior to ADP (Scheme 1). Interestingly, the *P. chrysogenum* APS kinase (13, 14) as well as the *Arabidopsis thaliana* (15), human (9), and rat (16, 17) enzymes have been reported to exhibit pronounced uncompetitive substrate inhibition by APS. Kinetic data suggest that the inhibitory complex results from formation of the *E*·ADP·APS complex (Scheme 1). In contrast, the APS kinase from *Escherichia coli* represents a distant protein that proceeds through a phosphorylated enzyme intermediate and exhibits competitive substrate inhibition (18). The physiological relevance of strong substrate inhibition observed in APS kinase is still ambiguous.

Crystal structures of APS kinases have been characterized for the *P. chrysogenum* (7, 19) and human enzymes (8, 20). For the latter, structures both in the context of the bifunctional protein (8) as well as of the isolated domain (20) have been reported. The *P. chrysogenum* enzyme (7, 19), the isolated human APS kinase domain of PAPSS1 (20), and the recently deposited structure of the APS kinase domain of PAPSS2 (PDB ID 2AX4) are found as a symmetrical dimer in the crystal, with the identical set of nucleotides present in the two monomers. In contrast, the crystallized bifunctional enzyme PAPSS1 (8) revealed an asymmetrical dimer, where one subunit had ADP bound (and APS after soaking), whereas the other subunit had no nucleotides in the active site. This difference raised the question of whether dimer asymmetry of the APS kinase domain in the context of the bifunctional enzyme is a crystallization artifact or a reflection of a real conformation in solution. Harjes *et al.* (8) rationalized the asymmetry to be a consequence of the differences in the P-loop sequence present in the human enzyme *versus* the one in the *P. chrysogenum* enzyme, which crystallized as a symmetrical dimer. However, our recent structure of the APS kinase domain from human PAPSS1 (20) shows a symmetrical dimer, thereby eliminating the sequence differences as a possible cause for the observed asymmetry.

Our structures of the APS kinase domain also reveal that the N-terminal region of one monomer is in close proximity to the active site of the other monomer (20). We designed several mutations in this region to investigate if this conformation is significant and if the N termini play a role in the catalytic activity of the enzyme. However, mutations of N-terminal residues closest to the active site had no effect on the activity (20). Surprisingly, it was found that, in a variant lacking the first 50 N-terminal residues (Δ50N), substrate inhibition was abolished and the maximum activity was approximately one-half compared with the full-length enzyme. To explain this unexpected result at the molecular level we solved the crystal structure of the Δ50N-truncated APS kinase domain variant of PAPSS1. Based on analysis of our structure we propose a model for the regulation of substrate inhibition that was validated by mutagenesis. Together, the work presented herein analyzes the nature and regulation of uncompetitive substrate inhibition observed in APS kinases, which contributes to the understanding of substrate inhibition *per se* and suggests a possible communication mechanism between the APS kinase and ATP-sulfurylase domains in the bifunctional PAPSS.

EXPERIMENTAL PROCEDURES

Protein Expression and Purification—The APS kinase domain (amino acid residues 25–227) of the PAPSS1 coding region (21) was cloned as a glutathione *S*-transferase fusion in the bacterial expression vector pGEX-RB (22) in which the thrombin cleavage site was replaced by a tobacco etch virus (TEV) protease recognition site. The same was done for the deletion mutant Δ34N-(35–227) and the point mutants R37A and R40A (the latter made in the background of the 25–227 construct). Proteins were expressed and purified as described before (20).

The deletion mutant Δ50N-(51–227) was initially cloned in the same vector as the other constructs, but the GST tag could not be effectively removed from the expressed protein. To overcome this problem, we cloned the 50–227 coding region of human APS kinase domain in the pJC20 vector that carries no tags. Transformed cells of the BL-21 Codon-Plus (Stratagene) strain of *Escherichia coli* were induced with 0.5 mM isopropyl 1-thio-β-D-galactopyranoside and left to grow at 22 °C overnight. Cells were lysed by sonication, and after centrifugation the supernatant was subjected to ammonium sulfate precipitation. Fractions precipitated with 40–80% of ammonium sulfate were pooled, resuspended, and dialyzed against a buffer containing 25 mM Tris, pH 7.5, 1 mM EDTA, 5 mM $MgCl_2$, and 2 mM dithiothreitol. The protein solution was applied on pre-equilibrated Blue-Sepharose 6 Fast Flow column (Amersham Biosciences), washed, and eluted with a salt gradient from 0 to 1 M KCl. Fractions eluted with 250–400 mM KCl were collected, merged, concentrated, and dialyzed against the same buffer as after ammonium sulfate precipitation. The protein was further purified by an anion exchange column (WP-QUAT, J. T. Baker, Phillipsburg, NJ) and highly pure Δ50N APS kinase eluted at 1 M KCl. Purified protein was dialyzed against 50 mM Tris, pH 7.5,

200 mM KCl, 5 mM dithiothreitol, and 5% glycerol, and stored at −80 °C. During the purification process the purity of APS kinase was followed by SDS-PAGE. The final yield from a 2-liter culture was ~8 mg of protein. Prior to crystallization, the Δ50N APS kinase protein was dialyzed against a solution containing 25 mM Tris-HCl, pH 7.5, 25 mM KCl, and 5 mM dithiothreitol.

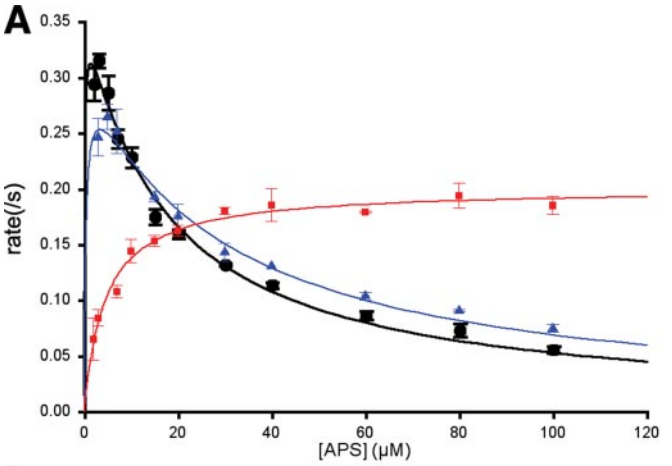

B

	k_{cat} (s^{-1})	K_m (μM)	K_i (μM)
WT	0.364 ± 0.024	< 2	17 ± 2
Δ34N	0.315 ± 0.025	< 2	29 ± 4
Δ50N	0.200 ± 0.004	4.6 ± 0.4	no inhibition

FIGURE 1. **The Δ50N APS kinase variant is devoid of APS substrate inhibition.** *A*, plot of initial rates as a function of APS concentration at constant 1 mM MgATP. Kinetic curves for the full-length wild-type-(1–227), the Δ34N-(35–227), and the Δ50N-(51–227) APS kinase constructs of human PAPSS1 and are shown in *black*, *blue*, and *red*, respectively. *B*, steady-state kinetic constants for the enzyme variants displaying substrate inhibition were obtained by fitting the curves to the equation, $v = V_{max}/(1 + K_m/[APS] + [APS]/K_i)$. That lacking substrate inhibition (*i.e.* Δ50N variant) was fitted to the Michaelis-Menten equation. *Colors* correspond to those in *A*.

Crystallization and X-ray Data Collection—Crystals were grown at room temperature using hanging drops containing equal volumes of protein and reservoir solution (2 + 2 μl). The protein solution contained 3.2 mg/ml Δ50N APS kinase, 2 mM dADP, 2 mM APS (or 2 mM PAPS), and 5 mM $MgCl_2$, whereas the reservoir contained 16–20% (w/v) polyethylene glycol 3350 and 0.25–0.15 M di-ammonium hydrogen citrate (pH 5.0). We used dADP instead of ADP to allow unambiguous discrimination to APS, which is isosteric to ADP. Nice single crystals appeared within 2 days and exceeded the size of 150 × 200 × 100 μm. 100% mineral oil (light white; Sigma M3516) was used as a cryoprotectant.

Data were collected using the SER-CAT beam line at the Advanced Photon Source, Argonne National Laboratories, and processed with the XDS program package (23).

Steady-state Kinetics—The APS kinase enzymatic assay in the forward reaction was performed by monitoring the rate of ADP formation using the pyruvate kinase/lactate dehydrogenase-coupled spectrophotometric assay that measures the decrease in absorbance at 340 nm due to the oxidation of NADH. The assay was performed using 200–400 nM enzyme in a buffer containing 50 mM Tris-HCl, pH 7.5, 100 mM KCl, 2.5 mM $MgCl_2$, 0.25 mM EDTA, 1.0 mM ATP, 0.4 mM phosphoenolpyruvate, and 0.2 mM NADH. The concentration of APS was varied between 2 and 100 μM. The reaction mixture was left to equilibrate for 10 min at 37 °C to allow for the consumption of trace ADP present in the ATP stock solution. APS kinase was added to trigger the reaction. All measurements were made in

TABLE 1
Data collection and refinement statistics

	dADP·PAPS	dADP·APS
Data collection		
PDB ID	2pez	2pey
Beamline	APS, SERCAT-BM	APS, SERCAT-BM
Wavelength (Å)	1.000	1.000
Unit cell (Å)	$a = 44.09, b = 59.40, c = 139.02, \alpha = \beta = \gamma = 90$	$a = 43.43, b = 59.75, c = 138.92, \alpha = \beta = \gamma = 90$
Space group	$P2_12_12_1$	$P2_12_12_1$
No. molecules/a.u.	2	2
Resolution limit (Å)	30-1.40	20-1.88
Measured reflections	273,547	202,712
Unique reflections	64,712	29,201
Completeness (%; overall/last shell)	88.6/87.0[a]	97.1/82.7[b]
I/σI (overall/last shell)	15.73/4.31[a]	16.63/4.14[b]
R_{sym}[c] (overall/last shell)	5.8/36.2[a]	9.1/42.9[b]
Refinement		
Resolution limit (Å)	20-1.40	20-1.88
No. reflections (working/free)	57,725/6,493	26,048/2,915
R_{cryst}[d] (overall/last shell)	0.197/0.255[a]	0.209/0.332[b]
R_{free} (overall/last shell)	0.220/0.302[a]	0.253/0.389[b]
No. protein/water/nucleotide residues	334/340/3	329/172/3
Root mean square deviation from ideal geometry (Å)		
Bond length	0.013	0.012
Angle distances	1.937	1.487
Estimated coordinate error (Å)	0.076	0.165
Ramachandran plot statistics		
Residues in most favored regions	90.8%	92.4%
Residues in allowed regions	8.2%	6.9%
Residues in generously allowed regions	1.0%	0.7%
Residues in disallowed regions	0.0%	0.0%

[a] Last shell (dADP·PAPS) = 1.398–1.435 Å.
[b] Last shell (APS·APS) = 1.885–1.933 Å.
[c] $R_{sym} = \Sigma|I - \langle I\rangle|/\Sigma I$.
[d] $R_{cryst} = \Sigma||F_{obs}| - |F_{calc}||/\Sigma|F_{obs}|$, 10% randomly omitted reflections were used for R_{free}.

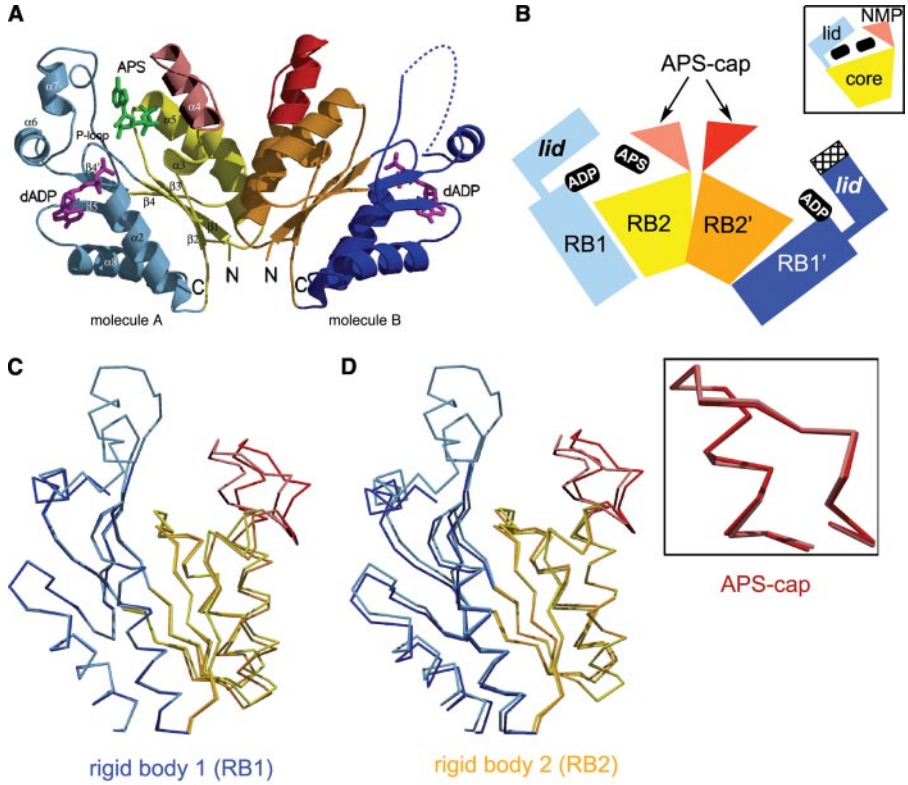

FIGURE 2. **The APS kinase domain consists of three rigid body parts.** *A*, a ribbon diagram of the dimeric Δ50N variant of the APS kinase domain from human PAPSS1 with dADP (*purple*) and APS (*green*) in the active site. Note that both nucleotides are present only in *molecule A*, whereas the active site of the *molecule B* contains only dADP. The empty phosphoryl acceptor binding site coincides with the disordered loop between helix α6 and strand β5 in molecule B. The Rigid Body 1 (*RB1*) region is shown in *light blue* in *molecule A* and *dark blue* in *molecule B*; Rigid Body 2 (*RB2*) is *yellow* in *molecule A* and *orange* in *molecule B*; the APS-cap regions are *pink* and *red* in *molecules A* and *B*, respectively. *B*, schematic of the Δ50N APS kinase dimer presented in the same color scheme as the ribbon diagram in *A*. *Inset*, schematic of an NMP kinase monomer demonstrates its similarity and difference to that of APS kinase. The three rigid bodies in NMP kinases are: lid (*blue*), core (*yellow*), and NMP binding region (*pink*). *C*, overlay of *molecule A* and *molecule B* of the Δ50N APS kinase variant based on Cα atoms belonging to residues that define RB1. Note the excellent overlay of RB1, and the different conformation of RB2 and APS-cap. *D*, analogous overlay as in *C* where Cα atoms from residues belonging to RB2 were used for calculating the superposition matrix. However, the APS-caps do not overlay well. Superposition of only APS-cap residues demonstrates that the APS-cap also behaves as a rigid body (*inset*). Together, *C* and *D* demonstrate the validity of dissecting APS kinase into three rigid bodies. *Colors* in *C* and *D* correspond to those in *A*.

triplicate at 37 °C using a Varian Cary 50 Bio UV-visible spectrophotometer.

RESULTS

Deletion of the 50 N-terminal Residues from the APS Kinase Domain of Human PAPSS1 Abolishes Substrate Inhibition—Previous work revealed that the N-terminal residues of the APS kinase domain of PAPSS1 form an extension that interacts with the neighboring molecule of the dimeric enzyme (20). Specifically, residues 26–35 of molecule A adopt an extended conformation near to the active site of molecule B (and *vice versa*), whereas residues 36–44 form a helix at the interface of the two molecules. Although the overall amino acid sequence conservation of the N-terminal region in APS kinase domains is low, two residues are highly conserved: an invariant asparagine at position 27, and either a glutamine or histidine at position 31. The proximity of these N-terminal residues of one molecule to its neighbor, together with sequence conservation at positions 27 and 31, suggested that these amino acids could be functionally important. To test this, point mutations and a deletion variant were generated. Surprisingly, the two point mutants (N27A and Q31A) as well as a variant lacking the first 34 N-terminal residues showed no appreciable effect on the enzyme kinetics (20). In contrast, deletion of additional 16 N-terminal residues (Δ50N mutant) resulted in a protein totally devoid of substrate inhibition by APS and with approximately half of the full-length's k_{cat} (Fig. 1). These results prompted us to solve the structure of the Δ50N variant of the APS kinase domain to decipher the structural reasons of the unexpected kinetic behavior observed for this construct. Our goal is to understand how the presence/absence of these 16 residues controls substrate inhibition.

Crystal Structure of Δ50N APS Kinase Domain of Human PAPSS1 Reveals an Asymmetrical Dimer—Structure of the Δ50N mutant of APS kinase domain (50–227) was solved in two different complexes. One complex contains dADP and APS, whereas the second has dADP and PAPS. The use of dADP instead of ADP in these studies allowed us to unambiguously differentiate between the isosteric nucleotides ADP and APS. Crystallographic data for the dADP·APS complex extended to 1.88 Å, and the structure was refined to an *R*-factor of 20.9% and R_{free} of 25.3%. The dADP·PAPS complex diffracted to 1.40 Å and was refined to an *R*-factor of 19.7% and R_{free} to 22.0%. Detailed data collection and refinement statistics for both complexes are summarized in Table 1.

The overall fold for the truncated enzyme (Fig. 2*A*) is essentially identical to that previously described for this domain in the context of the intact human bifunctional PAPSS1 (8) as well as the isolated APS kinase domain of PAPSS1 (20) and PAPSS2 (PDB ID 2AX4). However, where previously a symmetrical dimer was observed in the structures of the isolated domains in which both monomers had their nucleotide acceptor and nucleotide donor sites identically occupied, the Δ50N variant of APS kinase domain revealed an asymmetric dimer. One monomer has both nucleotides bound, as seen before, whereas the second monomer has only dADP present (*i.e.* APS or PAPS were absent). We observed the same asymmetrical dimer for both the dADP·APS and dADP·PAPS complexes reported here (see supplemental data). Interestingly, asymmetry within a dimer of the APS kinase domain has also been observed in the

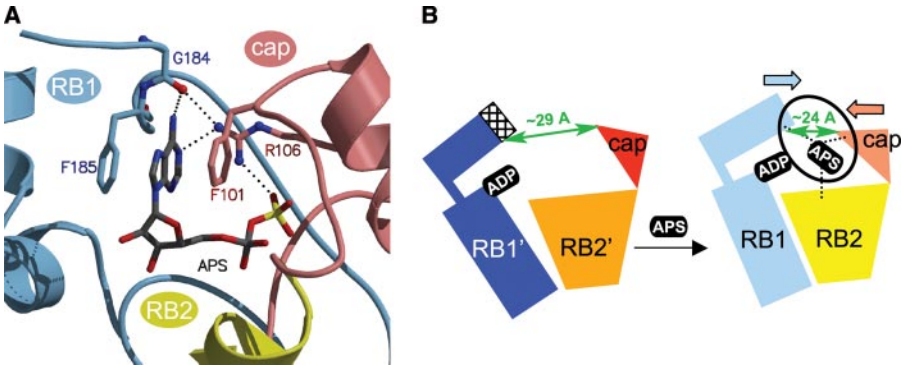

FIGURE 3. **Residues from all three rigid body domains participate in APS binding upon which a closed conformation is achieved.** *A*, binding of APS (in *ball-and-stick*) involves residues from all three rigid body regions: RB1 (*light blue*), RB2 (*yellow*), and APS-cap (*pink*). Specifically, the main chain carbonyl of Gly-184 from RB1 interacts with the guanidinium group of Arg-106 from APS-cap. The adenine base of the APS is further stabilized in a *syn* conformation through π-interactions provided by aromatic amino acids Phe-185 (*RB1*) and Phe-101 (*APS-cap*). RB2 residues contribute to APS binding by providing two NH main-chain interactions from residues Ile-132 and Ser-133 with the phosphate and sulfate moieties. For clarity, these interactions are omitted here but are shown in supplemental Fig. S2 together with all the interactions that were observed in the active site of *molecule A* of Δ50N APS kinase. *B*, schematic representing a monomer in the ADP-only bound state (as seen in *molecule B* of Δ50N APS kinase) on the *left* and in the ADP-APS-bound state (as seen in *molecule A*) on the *right*. The additional presence of APS in the active site results in the complete ordering of the RB1 lid region and in closure of the active site: the distance between the lid residue Gln-167 and APS-cap residue Ser-102 shrinks from 29 to 24 Å (*green arrow*).

context of the human bifunctional PAPSS1 (8). In that structure, one monomer had ADP bound (and APS after soaking) but the other monomer's active site remained invariably empty.

The absence of nucleotide in the phosphoryl acceptor-binding site of one monomer in our structures resulted in a flexible lid region, inferred by the lack of electron density for residues 171–190 in that monomer (*dashed line*, Fig. 2*A*; schematically represented as a *mesh pattern* in Fig. 2*B*). Lack of electron density for this segment of the protein in the absence of APS is consistent with prior results (8, 19). Detailed descriptions of the interactions made by the nucleotides and the enzyme are similar to those reported before and are presented as supplementary information (supplemental Fig. S2).

It has been noted by MacRea *et al.* (19) that the overall fold of APS kinase resembles that of the nucleoside monophosphate (NMP) kinases. These enzymes phosphorylate nucleoside 5′-monophosphates (*e.g.* AMP and GMP) to yield nucleoside 5′-diphosphates (*e.g.* ADP and GDP). Because APS kinase also catalyzes phosphoryl transfer, although this time to the ribose 3′-hydroxyl of APS to yield PAPS, it is not surprising that APS kinase adopts an "NMP kinase-like" fold.

Structural studies of NMP kinases revealed that these enzymes possess three regions named core, lid, and the NMP-binding region. In NMP kinases, these structural and functional elements behave as rigid bodies that change positions relative to one another during the catalytic cycle (24–26). We were able to also identify rigid regions in the APS kinase domain by comparing the two molecules present in the asymmetric unit: one with only dADP bound, the second with both dADP and APS. We included for this comparison other published structures of the human APS kinase domain (8, 20). The rigid regions present in APS kinase (Fig. 2*B*) are somewhat different from those identified for NMP kinases (*inset*, Fig. 2*B*). A part that was attributed to the core region in NMP kinases unites with the lid region in APS kinase (*blue colors*, Fig. 2) to form a region we call Rigid Body 1 (RB1) (Fig. 2*C*). The remaining part of the core (*yellow* and *orange*, Fig. 2) forms an independent rigid body that we designate as Rigid Body 2 (RB2) (Fig. 2*D*). The third rigid region in APS kinase (*inset*, Fig. 2*D*), the analogous part to the NMP-binding region of NMP kinases, is labeled APS-cap and is shown in *pink/red* in Fig. 2.

Comparison of the two monomers present in the crystal structure of the Δ50N variant reveals intramolecular differences (*i.e.* different relative orientations of RB1, RB2, and APS-cap). These differences can be attributed to the absence of APS in one of the monomers. In addition, superpositioning the structure of the APS kinase domain, which exhibits APS inhibition (residues 25–227), with the Δ50N variant reported here, which lacks APS inhibition, reveals intermolecular differences. The *intramolecular changes* (*i.e.* the relative orientation of the rigid regions within a monomer) and the *intermolecular changes* (*i.e.* the relative orientation of the two monomers forming the dimer) are related and are discussed in the next section.

Intramolecular Rearrangements, Closing of the Active Site—The APS kinase reaction follows the sequential ordered binding mechanism (Scheme 1) in which ATP binds prior to APS and PAPS leaves before ADP (13). To understand the intramolecular conformational changes that occur upon nucleotide binding we compared the nucleotide-free monomer of the APS kinase domain as observed by Harjes *et al.* (8) with our Δ50N monomer in which only dADP is present. We then added to our analysis the second Δ50N monomer (monomer A) where dADP occupies the phosphoryl-donor site and APS the acceptor site.

Superposition of the ligand-free APS kinase monomer and the dADP-only monomer shows that dADP binding, used here to approximate ATP binding, elicits only moderate conformational changes. These changes are mainly limited to the RB1 region. Specifically, rearrangements of the P-loop and the loop connecting β5 and α8 that provides the binding pocket for the adenine base take place. Most notably, binding of dADP orders 10 residues of the lid region (161–170), which in the absence of nucleotides has 31 unstructured residues (161–190; see Fig. S1). The lid residues adopt a more rigid conformation due to the stacking interaction between Arg-168 and the adenine base of dADP (supplemental Fig. S2). This decrease in flexibility of the lid region is necessary for effective binding of the second nucleotide APS, which would explain the obligate order of binding of this enzyme (13). Note that, although the binding of ATP with its associated magnesium ion would also induce a change in conformation of the DGDN-loop (for a discussion on the impact of magnesium binding to APS kinase see Ref. 20), which is a Walker B motif located in RB2, this change is not predicted

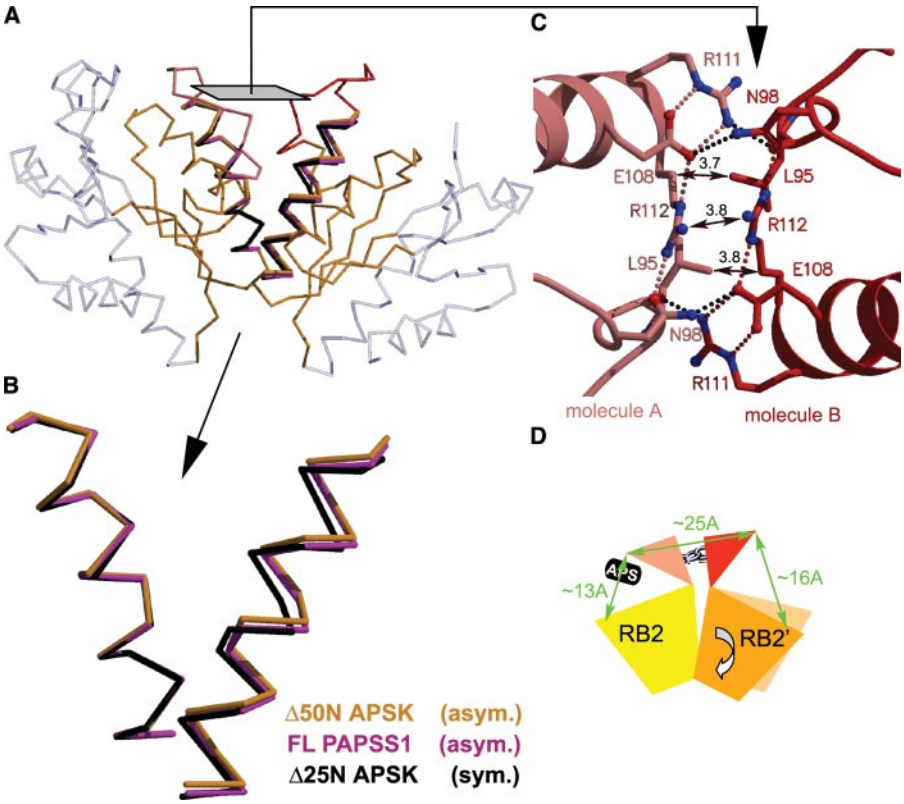

FIGURE 4. **Intermolecular rearrangements in the APS kinase dimer, the RB2 domains twist while the APS-caps remain tightly connected.** *A*, Cα trace of the Δ50N APS kinase dimer with the RB2 regions shown in *orange*, and the APS-cap regions from *molecules A* and *B* in *pink* and *red*, respectively. The RB1 regions are shown as *transparent blue objects*. Helix α4 of the RB2 region is shown as a *thicker object*. The corresponding α4 helices as observed in the structure of the full-length PAPSS1 (*magenta*) and in the Δ25N APS kinase variant (*black*) are superimposed. *B*, close-up view of helices α4 from the RB2 regions belonging to the two monomers that build the dimer. The overlay was done based only on Cα atoms in the helix belonging to molecule A. A twist between two α4 helices from asymmetrically crystallized complexes (Δ50N APS kinase (*orange*) and full-length PAPSS1 (*magenta*)) is obvious in comparison to the symmetrically crystallized Δ25N APS kinase (*black*). For clarity we show only the α4 helices, but the twist affects the entire RB2 region. *C*, a perpendicular view to the interactions maintained between the APS-cap regions belonging to *molecules A* and *B*. Intramolecular salt bridges are shown as *pink* and *red dotted lines*, whereas those made between the two monomers are in *black*. Hydrophobic interactions across the dimer interface (specifically π-interactions between the guanidinium groups of arginines 112 and between the Cγ atom of Arg-112 and Cδ atom of Leu-95) are presented as *black arrows* with the corresponding distances in Å. *D*, schematic representation of the dimer interface composed of the RB2 regions and APS-caps. The distance between the APS-cap of monomer A and that of monomer B, as measured with respect to Ser-102, is the same in both the symmetrical and asymmetrical dimer (~25 Å). In the symmetrical dimer the distance between APS-cap residue Ser-102 and RB2 residue Ile-132 is the same in both monomers (~13 Å). In contrast, in the asymmetrical Δ50N dimer, it increases by ~3 Å. This increase in distance is a consequence of the RB2 domain twisting.

to dramatically impact the relative orientation of the two rigid bodies RB1 and RB2.

Comparison of the dADP-bound APS kinase (*molecule B*, Fig. 2*A*) and the dADP·APS-bound enzyme (*molecule A*, Fig. 2*A*) reveals that the binding of APS generates a rearrangement of the domains RB1, RB2, and APS-cap. Interestingly, APS makes interactions with the lid (a component of RB1), in addition to interacting with the APS-cap and residues located in RB2 (Fig. 3*A* and supplemental Fig. S2). In particular, the adenine base is held firmly between Phe-185 from the lid (RB1) and Phe-101 from the APS-cap. Also, the main-chain carbonyl of the lid residue Gly-184 establishes interactions with the amino group of the adenine and with the APS-cap residue Arg-106, which is bridging between the sulfuryl group and the adenine moiety of APS. Such lid-phosphoryl acceptor interactions are not observed in NMP kinases, where the lid residues are only involved in phosphoryl-donor binding (usually ATP) and provide residues for phosphoryl transfer. In APS kinase, in addition to those roles, lid residues are engaged in the shaping of the phosphoryl-acceptor (APS) binding site. This property underscores the need for ordered binding where ATP must bind first to initiate the positioning of lid residues that would later participate in APS binding.

Most importantly, due to the interactions between the RB1 (lid), RB2, and the APS-cap, binding of APS, in addition to inducing local conformational changes, also changes the relative orientation of these regions. The latter results in a shortening of the distance between RB1 and RB2 and thus a "closing" of the APS kinase active site (Fig. 3*B*). Most pronounced is a reduction of the separation between the lid and APS-cap, decreasing by ~5 Å (measured between residue 102 of the APS-cap and 167 of the lid; *green arrow* Fig. 3*B*).

Intermolecular Rearrangements, Twisting between the Monomers—The presence of an asymmetrical dimer in the Δ50N structures prompted us to compare it to the symmetrical dimers observed for the slightly longer Δ25N variant. We noticed that when the RB2 regions from these two crystal structures are overlaid, the RB2′ regions (RB2′ designates the RB2 region of the other monomer) do not overlay well (Fig. 4, *A* and *B*). In contrast, if we perform the analogous overlay of Δ50N on the asymmetrical dimer of the APS kinase domain of human bifunctional PAPSS1 (8), the RB2′ regions overlay almost perfectly. In other words, the relative orientation of the two molecules forming the dimer is similar between the structures that exhibited asymmetry, but different to the symmetrical dimer.

This difference in quaternary conformation can be described as a 15° twist, as calculated by DynDom (27), between the two monomers that build the dimer. Although the monomer-monomer interface includes residues from both RB2 and the APS-cap, the twist motion involves only RB2. The relative orientation of the two APS-caps remains static due to the strong interactions between them (Fig. 4*C*). Similar interactions that "lock" the APS-cap regions from the two monomers were also reported for the *P. chrysogenum* APS kinase (19).

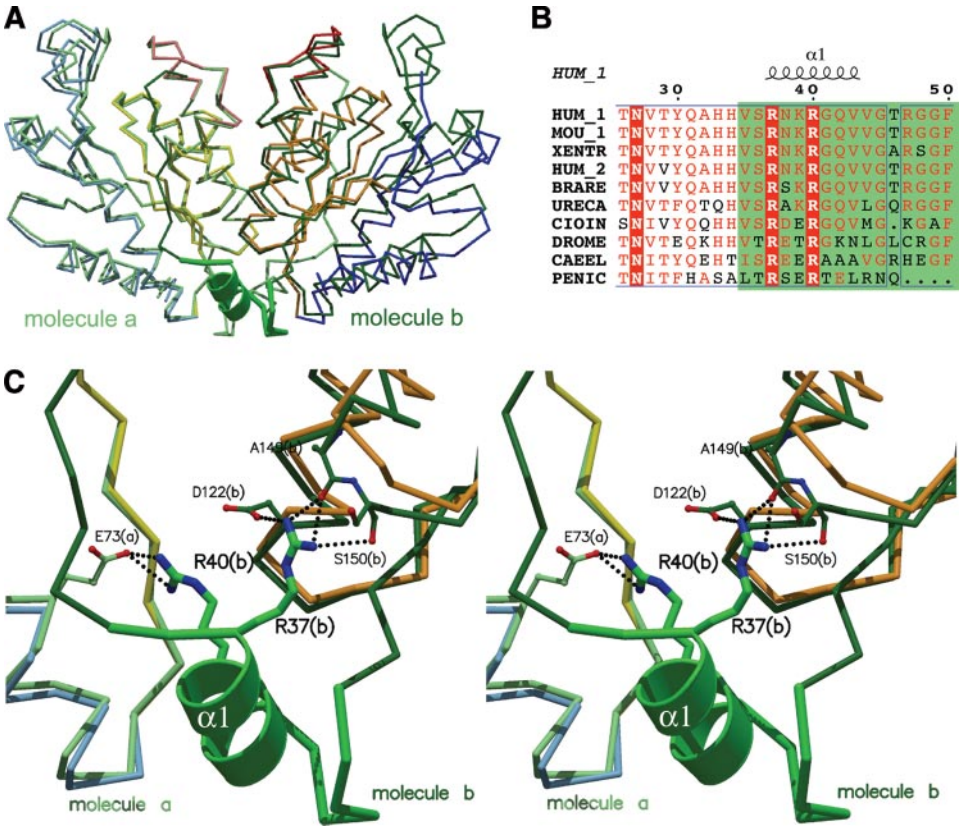

FIGURE 5. **Helix α1 plays a critical role in stabilizing a symmetrical dimer.** *A*, overlay of the symmetrical Δ25N and asymmetrical Δ50N dimer of APS kinase based on the Cα atoms from the RB2 domain of *molecule A*. Rigid body regions of the Δ50N variant are *colored* as in Fig. 2, while monomers A and B of the Δ25N enzyme are in *light* and *dark green*, respectively. The slight differences between *molecules A* show that the closed conformation of the symmetrical dimer is somewhat more closed than that in the asymmetrical dimer. The large differences between *molecules B* shown are a result of the opening of the molecule due to the lack of APS in the Δ50N structure, and of the ensuing twist motion of this molecule's RB2 region. *B*, sequence alignment of the N-terminal region present in several bifunctional (*HUM_1*, human PAPSS1; *MOU_1*, mouse PAPSS1; *XENTR*, *Xenopus tropicalis* PAPSS; *HUM_2*, human PAPSS2; *BRARE*, *Brachydanio rerio* PAPSS; *URECA*, *Urechis caupo* PAPSS; *CIOIN*, *Ciona intestinalis* PAPSS; *DROME*, *Drosophila melanogaster* PAPSS; and *CAEEL*, *Caenorhabditis elegans* PAPSS) and monofunctional (*PENIC*, *P. chrysogenum*) APS kinases. Residues present in the Δ34N construct but missing from the Δ50N construct are highlighted in *green*. Note the low conservation in this area with the exception of the two arginine residues, Arg-37 and Arg-40, in the helix α1. *C*, stereo representation showing the interactions of arginines 37 and 40. Arg-40 from the α1 helix belonging to *molecule B* interacts with the carboxylic group of Glu-73 from the RB1 of *molecule A*. Arg-37 from *molecule B*, on the other hand, makes bidentate interactions with main-chain carboxyls of Ala-149 and Ser-150, as well as with the carboxyl moiety of the Asp-122, all belonging to RB2 of the same molecule (*molecule B*). In this way, helix α1 of *molecule B* connects RB1 of *molecule A* and RB2 of *molecule B*. Residues are labeled with *one-letter code* and *sequence number*. Chain designation is noted in *parenthesis*.

As a consequence of this movement, RB2′ shifts away from the APS-cap (see *schematic*, Fig. 4*D*). The RB2-APS-cap separation, as measured between residues 132 (RB2) and 102 (APS-cap), increases by ~3 Å. Because APS binding requires residues from both the APS-cap and RB2 regions, the resulting conformation of this monomer has a distorted APS-binding site.

Role of the α1 Helix—As was mentioned before, deletion of the first 34 N-terminal amino acids results in an enzyme with similar kinetic behavior to the full-length domain, whereas deletion of additional 16 residues (Δ50N construct) yields an enzyme devoid of substrate inhibition. We focused on the interactions established by these 16 residues (shown as a *thick green ribbon* in the Fig. 5*A*) to understand how these residues are involved in APS substrate inhibition.

The most prominent structural element constructed by these residues is helix α1. Interestingly, although most of the residues comprising this helix are not conserved, two arginines are strictly conserved: Arg-37 and Arg-40 (Fig. 5*B*). Arg-37 forms salt bridges with two RB2 residues from the *same monomer*: the side chain of Asp-122 and main-chain carbonyl of Ser-150. On the other hand, Arg-40 forms a salt bridge with the side chain of Glu-73, which is an RB1 residue from the *opposite monomer* (Fig. 5*C*). Thus, helix α1 arginine residues build ionic interactions between RB1 of the one molecule and RB2 of the other molecule. Because the relative orientation of RB1 to RB2 changes upon APS binding (see intramolecular movements above), and because helix α1 connects these two regions, albeit between neighboring molecules, we speculated that the absence of these interactions in the Δ50N enzyme could rationalize the lack of APS inhibition of the truncated enzyme.

To explore this possibility we mutated each of these arginines to alanine in the full-length background and kinetically characterized these mutants (Fig. 6). Consistent with our model, the R37A and the R40A mutants did not show APS inhibition, and were, in fact, kinetically indistinguishable from the Δ50N variant. This demonstrates that the interactions established by arginines 37 and 40 are indispensable for maintaining substrate inhibition of the APS kinase domain in human PAPSS1.

DISCUSSION

APS kinases are characterized by having an ordered sequential mechanism and a strong substrate inhibition of APS (9, 13, 15, 17) (see Scheme 1). Our previous work (20) on the isolated APS kinase domain of human PAPSS1 revealed that the N terminus of one molecule approaches the active site of the second molecule that builds the functional dimeric enzyme. Protein engineering experiments probing for the exact function of these N-terminal amino acids revealed that residues 36–50 are required for the APS substrate inhibition. To understand why the lack of these residues abolishes substrate inhibition, we solved the crystal

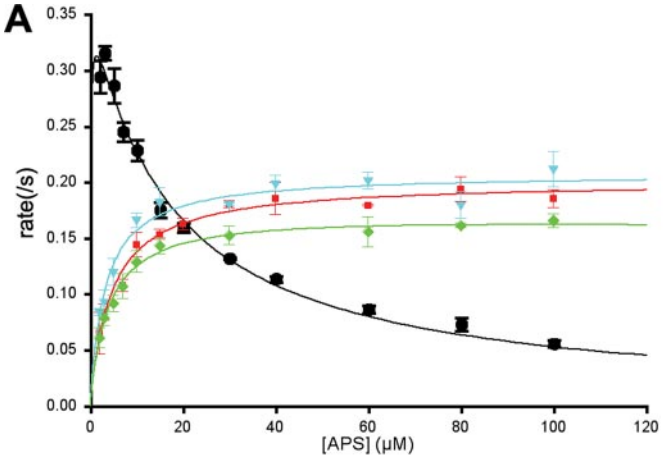

B

	k_{cat} (s^{-1})	K_m (μM)	K_i (μM)
WT	0.364 ± 0.024	< 2	17 ± 2
Δ50N	0.200 ± 0.004	4.6 ± 0.4	no inhibition
R37A	0.207 ± 0.004	3.2 ± 0.4	no inhibition
R40A	0.170 ± 0.003	3.7 ± 0.3	no inhibition

FIGURE 6. **The R37A and R40A mutants, like the Δ50N construct, are devoid of substrate inhibition.** *A*, initial rates for the full-length (*black*), Δ50N (*red*), R37A (*cyan*), and R40A (*green*) APS kinase of human PAPSS1 are shown as a function of APS concentration at constant 1 mM MgATP. Note that for comparison purposes the curves for the full-length and Δ50N constructs are duplicated from Fig. 1. *B*, steady-state kinetic constants for the four enzyme variants were obtained by fitting to the equations as in Fig. 1. *Colors* correspond to those in *A*.

structure of a Δ50N variant of the APS kinase domain in complex with dADP and APS and with dADP and PAPS.

The first surprising finding was that this N-terminally truncated enzyme crystallized in an asymmetric fashion, where molecule A had both nucleotides present (*i.e.* dADP and APS or PAPS), whereas molecule B contained only dADP. This was unexpected, because the previously reported structures of the APS kinase domain of PAPSS1 (20) (residues 25–227) and PAPSS2 (residues 21–218; PDB ID 2AX4) crystallized in a symmetric fashion. We asked if the observed asymmetry in the structure could be a direct consequence of the absence of the N-terminal residues. To answer this, we first performed an analysis of the rigid domains present in APS kinases. We compared the conformation of the ligand-free monomer (8) to that where only dADP is bound (*monomer B*, Fig. 2), and finally to where both dADP and APS are bound (*monomer A*, Fig. 2). This analysis identified the three rigid body domains that build each APS kinase monomer, termed RB1, RB2, and APS-cap. These domains change their relative orientation in response to the binding of the nucleotides. In addition to these intramolecular changes, we identified a change in the quaternary structure of the APS kinase dimer. In other words, the relative orientation of the two monomers that form the symmetrical dimer (20) is different to that of the asymmetrical dimer (Ref. 8 and that reported here). We propose that this difference has ramifications on the ability of the enzyme to utilize both active sites simultaneously (see below).

Comparison of the nucleotide-free enzyme with the dADP-bound form reveals that the binding of nucleotide at the phosphoryl donor site primes the lid region to complete its additional role of complexing APS. In the absence of this priming, APS cannot bind to the enzyme. Notably, according to our analysis, binding of nucleotide to the phosphoryl donor site of the apo-enzyme does not significantly alter the relative orientations of the rigid bodies.

Upon subsequent APS binding at the cleft between the lid and APS-cap, the entire lid region becomes ordered. Additionally, the whole RB1 domain and the APS-cap move closer to RB2 as APS stabilizes a more closed conformation. Thus, binding of APS involves interactions from all three rigid bodies (RB1, RB2, and APS-cap) and results in their reorientation within the monomer.

Overlay of the symmetrical APS kinase dimer (20) on the here reported asymmetrical dimer reveals a slightly different inter-monomer orientation. This difference, which we refer to as a twist, affects the whole RB2 region. The APS-cap also makes numerous intermolecular interactions. In contrast to the RB2 region, the relative orientation of the two APS-caps is maintained regardless of the molecules forming a symmetric or asymmetric conformation.

With this information, we can address the question of why the Δ50N variant displays the asymmetrical dimer whereas the full-length enzyme adopts a symmetric form. The truncated enzyme is missing helix α1. This helix in the full-length enzyme connects the RB2 region of the monomer that it is a part of, and the RB1 of the other monomer (Fig. 7*A*). In its absence, the coupling between RB1-RB2′ (and RB1′-RB2) is lost, and this allows the RB2 region of one monomer to twist relative to the other monomer. The twist motion results in an opening of one monomer in the dimer, where the relative distance between RB1 and RB2 is increased. As a result of this opening of the monomer, the affinity for APS is diminished. In total, the twist allows for only one monomer to have both nucleotides bound in the active site, and the other monomer has just the nucleotide in the phosphoryl-donor binding site. The ultimate result therefore is an asymmetrical dimer (Fig. 7*B*, *panel i*).

In the above model, we propose a coupling function between the two monomers carried out by the α1 helix. Analysis of the structures revealed that two conserved arginines in the helix play an important part here: Arg-37 connects the α1 helix to its RB2 domain, whereas Arg-40 connects it to the RB1 of the second monomer. Indeed, mutating these arginines into alanines totally abolishes substrate inhibition, consistent with the predicted role for these residues.

The lack of intermolecular interactions provided by helix α1 serves to explain the lack of substrate inhibition as well as reduced k_{cat} of the truncated APS kinase variant. In enzyme species containing helix α1 with arginines 37 and 40, a symmetrical dimer can be formed where all four nucleotide-binding sites can be occupied simultaneously. In such a situation, the inhibitory ADP·APS complex can be formed in each of the monomers (Fig. 7*A*). Upon deletion of the helix (*i.e.* Δ50N variant), or upon mutation of the critical arginines in this helix (*i.e.* R37A or R40A), the stabilizing function of this region is lost. The result is a twisting motion of RB2 regions in a dimer. However, the tight interactions connect-

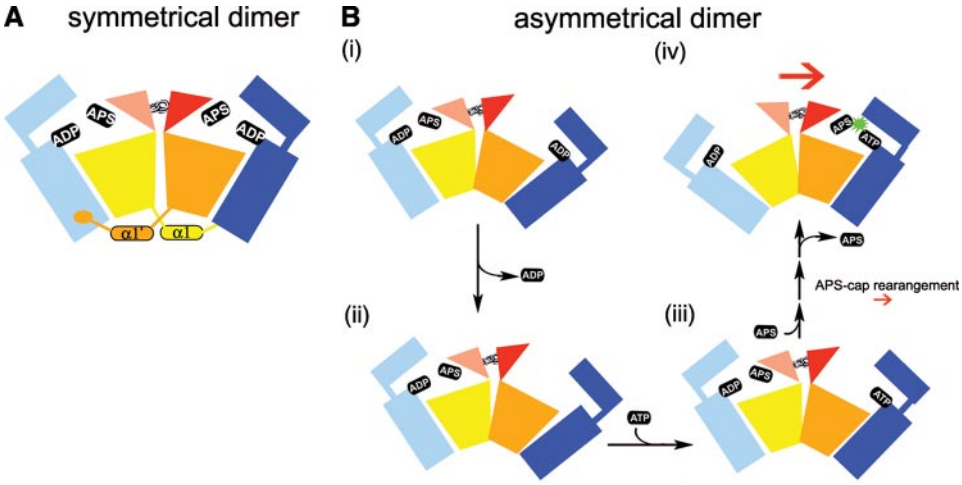

FIGURE 7. **Schematic model for the role of helix α1 in substrate inhibition.** *A*, in the presence of helix α1 the APS kinase can adopt a symmetric dimer. In such a state, both active sites can simultaneously bind APS and ADP, thereby forming an inhibitory complex. *B*, enzyme lacking helix α1 adopts an asymmetrical dimer in which one subunit has a non-functional APS-binding site. From this state (*i*), ADP can leave (*ii*), and ATP can bind (*iii*). To the *E*·ATP complex, the second substrate APS can bind resulting in a closed conformation for that monomer (*iv*). Concomitantly, the APS binding site of the neighboring molecule becomes non-functional, thereby eliciting APS release. See text for details.

ing the two APS-caps do not allow the APS-cap region to move in concert with the RB2 regions. Therefore, the APS-binding site in one monomer is distorted and we observe no APS in that site (Fig. 7*B*, *panel i*).

An important consequence of the diminished APS affinity in the twisted monomer, and hence the absence of APS, is that now ADP can easily leave this monomer (Fig. 7*B*, *panel ii*). Remember that, due to the ordered binding mechanism of APS kinase, APS release must occur before ADP can leave. The now nucleotide-free monomer is able to bind its first substrate ATP (Fig. 7*B*, *panel iii*). Subsequent binding of the second substrate APS attracts the APS-cap region so that a closed conformation forms. However, because the two APS-cap domains are tightly connected and RB2s are twisted, this closure in one monomer elicits a concomitant opening in the adjacent monomer. The now distorted APS-binding site in the previously closed monomer allows for APS dissociation from that monomer (Fig. 7*B*, *panel iv*).

To summarize our structural model, a dimer lacking a functional helix α1 cannot simultaneously bind all four nucleotides (two per monomer). In other words, the APS/PAPS-binding site can only be fully formed in one monomer at a time. The above model of the Δ50N-construct implies that the two active sites cannot be catalytically competent at the same time, just as they cannot be inhibited at the same time. Kinetic data showing that the k_{cat} of the Δ50N-variant is approximately half of the k_{cat} observed for the constructs having an intact helix α1, along with the lack of APS inhibition, support the proposed single-piston model.

The asymmetrical APS kinase dimer conformation we see for the Δ50N enzyme may be physiologically relevant based on the observation of similar asymmetry of the APS kinase domain in the context of the bifunctional PAPSS1 (8). For the bifunctional enzyme, asymmetry appears to be induced by interactions of an APS kinase monomer with an ATP-sulfurylase monomer. These interdomain (*i.e.* APS kinase with ATP-sulfurylase) interactions prohibit Arg-40 of the APS kinase domain from fulfilling its stabilizing role. Hence this monomer is subject to a similar twisting motion that we identified for the Δ50N APS kinase construct. The end result is a more open monomer that is not competent for nucleotide binding.

In summary, our studies of the Δ50N APSK variant of human PAPSS1 reveal the structural elements involved in potent APS substrate inhibition and advance a model for its regulation. Furthermore, our analysis suggests that the ATP-sulfurylase domain can act to modulate the activity of the APS kinase domain by interactions that affect the function of helix α1 of the kinase domain. So, although the crystal structure of the intact PAPSS1 does not support substrate channeling between the two enzyme domains, our results suggest a model for pronounced communication between domains.

Acknowledgments—We thank the staff of South East Regional Collaborative Access Team for assistance in data collection. We are grateful to Stephan Ort for help in construction of expression clones.

REFERENCES

1. Colletier, J.-P., Fournier, D., Greenblatt, H. M., Stojan, J., Sussman, J. L., Zaccai, G., Silman, I., and Weik, M. (2006) *EMBO J.* **25,** 2746–2756
2. LiCata, V. J., and Allewell, N. M. (1997) *Biophys. Chem.* **64,** 225–234
3. Xu, H., West, A. H., and Cook, P. F. (2006) *Biochemistry* **45,** 12156–12166
4. Klaassen, C. D., and Boles, J. W. (1997) *FASEB J.* **11,** 404–418
5. Venkatachalam, K. V. (2003) *IUBMB Life* **55,** 1–11
6. Beynon, J. D., MacRae, I. J., Huston, S. L., Nelson, D. C., Segel, I. H., and Fisher, A. J. (2001) *Biochemistry* **40,** 14509–14517
7. Lansdon, E. B., Segel, I. H., and Fisher, A. J. (2002) *Biochemistry* **41,** 13672–13680
8. Harjes, S., Bayer, P., and Scheidig, A. J. (2005) *J. Mol. Biol.* **347,** 623–635
9. Lansdon, E. B., Fisher, A. J., and Segel, I. H. (2004) *Biochemistry* **43,** 4356–4365
10. ul Haque, M. F., King, L. M., Krakow, D., Cantor, R. M., Rusiniak, M. E., Swank, R. T., Superti-Furga, A., Haque, S., Abbas, H., Ahmad, W., Ahmad, M., and Cohn, D. H. (1998) *Nat. Genet.* **20,** 157–162
11. Sugahara, K., and Schwartz, N. B. (1979) *Proc. Natl. Acad. Sci. U. S. A.* **76,** 6615–6618
12. Kurima, K., Warman, M. L., Krishnan, S., Domowicz, M., Krueger, R. C., Jr., Deyrup, A., and Schwartz, N. B. (1998) *Proc. Natl. Acad. Sci. U. S. A.* **95,** 8681–8685
13. Renosto, F., Seubert, P. A., and Segel, I. H. (1984) *J. Biol. Chem.* **259,** 2113–2123
14. MacRae, I. J., and Segel, I. H. (1999) *Arch. Biochem. Biophys.* **361,** 277–282
15. Lillig, C. H., Schiffmann, S., Berndt, C., Berken, A., Tischka, R., and Schwenn, J. D. (2001) *Arch. Biochem. Biophys.* **392,** 303–310
16. Hommes, F. A., Moss, L., and Touchton, J. (1987) *Biochim. Biophys. Acta* **924,** 270–275
17. Lyle, S., Geller, D. H., Ng, K., Stanczak, J., Westley, J., and Schwartz, N. B. (1994) *Biochem. J.* **301,** 355–359

18. Satishchandran, C., and Markham, G. D. (1989) *J. Biol. Chem.* **264,** 15012–15021
19. MacRae, I. J., Segel, I. H., and Fisher, A. J. (2000) *Biochemistry* **39,** 1613–1621
20. Sekulic, N., Dietrich, K., Paarmann, I., Ort, S., Konrad, M., and Lavie, A. (2007) *J. Mol. Biol.* **367,** 488–500
21. Venkatachalam, K. V., Akita, H., and Strott, C. A. (1998) *J. Biol. Chem.* **273,** 19311–19320
22. Brundiers, R., Lavie, A., Veit, T., Reinstein, J., Schlichting, I., Ostermann, N., Goody, R. S., and Konrad, M. (1999) *J. Biol. Chem.* **274,** 35289–35292
23. Kabash, W. (1993) *J. Appl. Crystallogr.* **26,** 795–800
24. Schulz, G. E., Muller, C. W., and Diederichs, K. (1990) *J. Mol. Biol.* **213,** 627–630
25. Sekulic, N., Shuvalova, L., Spangenberg, O., Konrad, M., and Lavie, A. (2002) *J. Biol. Chem.* **277,** 30236–30243
26. Segura-Pena, D., Sekulic, N., Ort, S., Konrad, M., and Lavie, A. (2004) *J. Biol. Chem.* **279,** 33882–33889
27. Hayward, S., and Berendsen, B. H. (1998) *Proteins* **30,** 144–154